nature medicine

A high-throughput drug screen for *Entamoeba histolytica* identifies a new lead and target

Anjan Debnath[1], Derek Parsonage[2], Rosa M Andrade[3,4], Chen He[3], Eduardo R Cobo[3], Ken Hirata[3], Steven Chen[5], Guillermina García-Rivera[6], Esther Orozco[6], Máximo B Martínez[6], Shamila S Gunatilleke[1], Amy M Barrios[7], Michelle R Arkin[5], Leslie B Poole[2], James H McKerrow[1] & Sharon L Reed[3,4]

***Entamoeba histolytica*, a protozoan intestinal parasite, is the causative agent of human amebiasis. Amebiasis is the fourth leading cause of death and the third leading cause of morbidity due to protozoan infections worldwide[1], resulting in ~70,000 deaths annually. *E. histolytica* has been listed by the National Institutes of Health as a category B priority biodefense pathogen in the United States. Treatment relies on metronidazole[2], which has adverse effects[3], and potential resistance of *E. histolytica* to the drug is an increasing concern[4,5]. To facilitate drug screening for this anaerobic protozoan, we developed and validated an automated, high-throughput screen (HTS). This screen identified auranofin, a US Food and Drug Administration (FDA)-approved drug used therapeutically for rheumatoid arthritis, as active against *E. histolytica* in culture. Auranofin was ten times more potent against *E. histolytica* than metronidazole. Transcriptional profiling and thioredoxin reductase assays suggested that auranofin targets the *E. histolytica* thioredoxin reductase, preventing the reduction of thioredoxin and enhancing sensitivity of trophozoites to reactive oxygen-mediated killing. In a mouse model of amebic colitis and a hamster model of amebic liver abscess, oral auranofin markedly decreased the number of parasites, the detrimental host inflammatory response and hepatic damage. This new use of auranofin represents a promising therapy for amebiasis, and the drug has been granted orphan-drug status from the FDA.**

Screening large chemical libraries to identify amebicidals has been hindered by the throughput of labor-intensive traditional assays that rely on microscopic visualization[6], radioisotopes[7] and/or extensive staining methods[8]. We developed and employed an automated HTS that is suitable for rapid and more efficient screening of large, diverse inhibitor libraries for activity against *E. histolytica*. The challenges of developing the HTS platform for *E. histolytica* included the facts that it is an anaerobe and that no rapid readout assay is available. We solved these issues by using GasPak EZ Anaerobe Gas Generating Pouch Systems and the CellTiter-Glo Luminescent Cell Viability Assay. The GasPak was not needed during robotic transfers, making this assay fully compatible with workstation-based automation. We developed the assay with exponentially growing *E. histolytica* trophozoites plated at 50,000 parasites per milliliter in 96-well[8] or 30,000 parasites per milliliter in 384-well microtiter plates. We maintained anaerobic conditions using GasPak during growth. As ATP is an essential cofactor for biogenesis in *E. histolytica*, we used the CellTiter-Glo luciferase-based assay to validate the correlation between the number of viable trophozoites and their ATP levels. The relationship between numbers of parasites seeded into 96- and 384-well plates and relative luminescence from CellTiter-Glo assaying of parasites showed a linear correlation ($R^2 = 0.86$ and $R^2 = 0.9$) (**Fig. 1a**,**b**). Trophozoites readily tolerated up to 0.5% DMSO, used to dissolve the compounds, with no effect on growth rate (data not shown). In our system, the half-maximal effective concentration (EC_{50}) for metronidazole, defined as that concentration of compound necessary to reduce the culture density to 50% of that of a DMSO-treated culture, was 5 μM. We used this HTS assay to evaluate the amebicidal activity of potential drug candidates, with parasites plated at 50,000 parasites per milliliter in a 96-well microtiter plate at a single concentration of 5 μM of the test compound.

We performed the screen with a 910-member Iconix library, consisting of both FDA-approved and unapproved bioactive compounds. The use of drugs already approved for human use opens the possibility to reprofile or repurpose[9] drugs to treat amebiasis in a rapid and cost-effective manner; using approved compounds allows for shortened development timelines and decreased risk, as such compounds have already passed regulatory clinical trials with full toxicological and pharmacokinetic profiles[9].

We identified 11 compounds as 'active', causing statistically significant growth inhibition (>50%; **Fig. 1c** and **Table 1**). The assay showed excellent discrimination between active and inactive compounds with a Z' (a dimensionless calculation used to assess the quality of a

[1]Sandler Center for Drug Discovery, University of California–San Francisco, San Francisco, California, USA. [2]Department of Biochemistry, Wake Forest School of Medicine, Winston-Salem, North Carolina, USA. [3]Department of Pathology, University of California–San Diego, San Diego, California, USA. [4]Department of Medicine, University of California–San Diego, San Diego, California, USA. [5]Small Molecule Discovery Center, University of California–San Francisco, San Francisco, California, USA. [6]Department of Experimental Pathology, Centro de Investigación y de Estudios Avanzados del Instituto Politécnico Nacional, Mexico City, Mexico. [7]Department of Medicinal Chemistry, University of Utah, Salt Lake City, Utah, USA. Correspondence should be addressed to S.L.R. (slreed@ucsd.edu) or A.D. (anjan.debnath@ucsf.edu).

Received 3 October 2011; accepted 30 March 2012; published online 20 May 2012; doi:10.1038/nm.2758

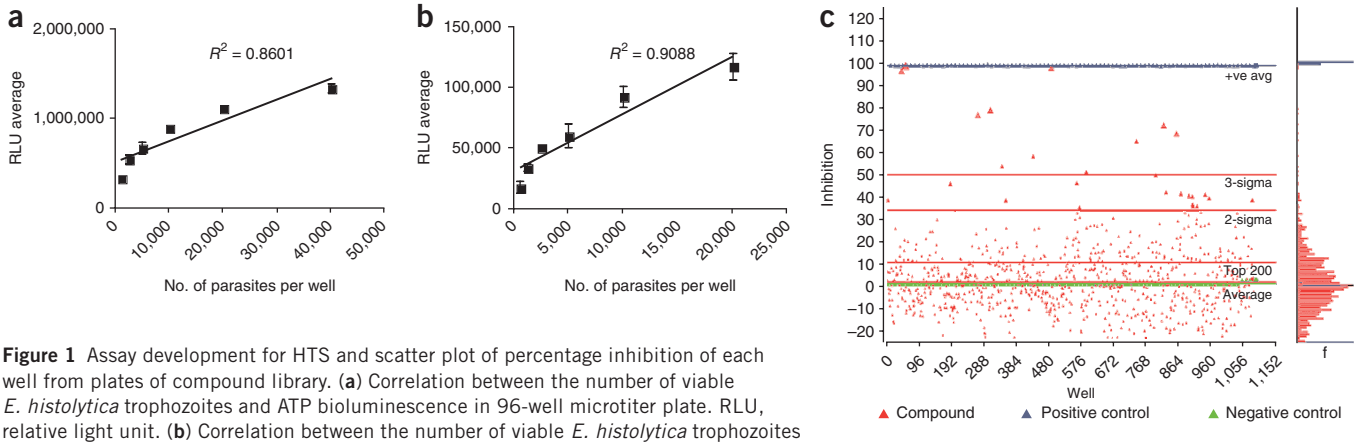

Figure 1 Assay development for HTS and scatter plot of percentage inhibition of each well from plates of compound library. (**a**) Correlation between the number of viable *E. histolytica* trophozoites and ATP bioluminescence in 96-well microtiter plate. RLU, relative light unit. (**b**) Correlation between the number of viable *E. histolytica* trophozoites and ATP bioluminescence in 384-well microtiter plate. Values plotted in **a** and **b** are the means and s.d. of triplicate wells. The lines represent the linear regression for plotted data. (**c**) Scatter plot of percentage inhibition of each well from 12 96-well plates of the Iconix library. Eleven compounds yielded both 50% inhibition and 3 s.d. above the mean of the population of compounds tested in the primary screen at 5 μM. +ve avg, mean inhibition of positive controls; 3-sigma, 50% inhibition and 3 s.d. above the mean of the population of compounds tested; 2-sigma, 2 s.d. above the mean of the population of compounds tested; top 200, top 200 active compounds above the mean of the population of compounds tested; average, mean of the population of compounds tested. Right graph represents the histogram of the compounds tested.

high-throughput assay) of 0.96 ± 0.13 in the screening experiment using 12 different plates containing the Iconix library compounds. Among the 11 compounds, auranofin had the highest amebicidal activity with an EC_{50} of 0.5 μM, tenfold better than that of metronidazole. Auranofin purchased from another manufacturer and three auranofin analogs also inhibited growth of *E. histolytica* trophozoites (**Supplementary Table 1**). Two purine analogs, cladribine and fludarabine, showed 79% and 77% growth inhibition, respectively, at 5 μM but are not promising for further development because of reported adverse effects in humans. We also identified trifluoperazine, a compound with known amebicidal activity[10], as a primary hit, confirming the sensitivity of our whole-cell HTS assay format.

Auranofin is an FDA-approved oral, gold-containing drug that has been in clinical use to treat rheumatoid arthritis for 25 years and is sold as Ridaura (Prometheus). The published pharmacokinetic data of auranofin come from studies in humans with rheumatoid arthritis after long-term therapy. Auranofin is rapidly metabolized, so only the released elemental gold can be detected in human blood or tissues. Following an oral dose, 25% of auranofin (gold) is absorbed into blood, of which 60% is bound by plasma proteins[11]. Steady-state mean blood gold concentrations in humans are 0.68 ± 0.45 μg ml^{-1} (according to the package insert from the manufacturer) or approximately 3.5 μM, more than 7 times the *in vitro* EC_{50} for *E. histolytica*. Auranofin was approved for the long-term treatment of unresponsive rheumatoid arthritis in adults with courses for a minimum of 6 months at oral doses of 3 mg once or twice daily (not adjusted for weight). The manufacturer indicates the following complications in patients treated for at least 1 year with auranofin: 47% of patients had at least one loose stool, 24% a rash, 14% an episode of abdominal pain, 13% stomatitis, 10% nausea, 3% anemia and 2% elevated liver function tests at some point. The likelihood of gold toxicity is extremely small in the standard, short-term (7–10 d) therapy for amebiasis.

Recently, auranofin has been shown to rapidly kill juvenile and adult *Schistosoma mansoni* in culture at concentrations achievable in patients with rheumatoid arthritis (5 μM)[12] and the bloodstream and procyclic stages of *Trypanosoma brucei* with half-maximal inhibitory concentration (IC_{50}) in the lower nanomolar range[13]. Concentrations as low as 2.5 μM also kill larval worms of *Echinococcus granulosus in vitro*[14]. Auranofin also strongly inhibits the growth of malarial parasite *Plasmodium falciparum in vitro*[15] and kills the promastigote stage of *Leishmania infantum in vitro* at micromolar concentrations[16].

Although auranofin has been used clinically for 25 years, its mechanism of action is poorly understood. To identify the basis of auranofin's activity against *E. histolytica*, we undertook a transcriptional profiling study using *E. histolytica* oligonucleotide microarrays[17]. Incubation of *E. histolytica* with 1 μM auranofin for only 3 h induced downregulation of genes encoding crucial proteins involved in mitosis (Rae1 (ref. 18)) and nucleotide metabolism (nucleoside diphosphate kinase[19]), whereas the genes encoding the signal transduction proteins ADP-ribosylation factor and Ras1p were upregulated[20] (**Supplementary Table 2**). However, these transcripts are also induced by other forms of cellular stress[21]. Furthermore, there was a marked upregulation of the gene encoding a protein similar to arsenite-inducible RNA-associated protein (AIRAP) (**Supplementary Table 2**). The differential expression of these down- and upregulated transcripts in auranofin-treated *E. histolytica* was validated by real-time quantitative reverse transcription PCR (qRT-PCR) (**Supplementary Fig. 1** and **Supplementary Table 3**).

AIRAP is unique among known arsenite-induced genes in that its expression is not upregulated in response to other oxidants and is only modestly induced by exposure to metals, such as zinc[22], although gold has not been tested. Our finding that the transcript for a gene similar to that encoding AIRAP in *E. histolytica* was highly upregulated by treatment with low concentrations of auranofin thereby identifies a

Table 1 Hits obtained after screening the Iconix library

Compound	Percentage inhibition (5 μM)
Auranofin	100
Sporidesmin A	99
Cycloheximide	98
Cladribine	79
Fludarabine	77
Homochlorcyclizine	73
Trifluoperazine	69
Idarubicin	65
4,4′-diethylaminoethoxyhexestrol	58
Clomiphene	54
Amiodarone	51

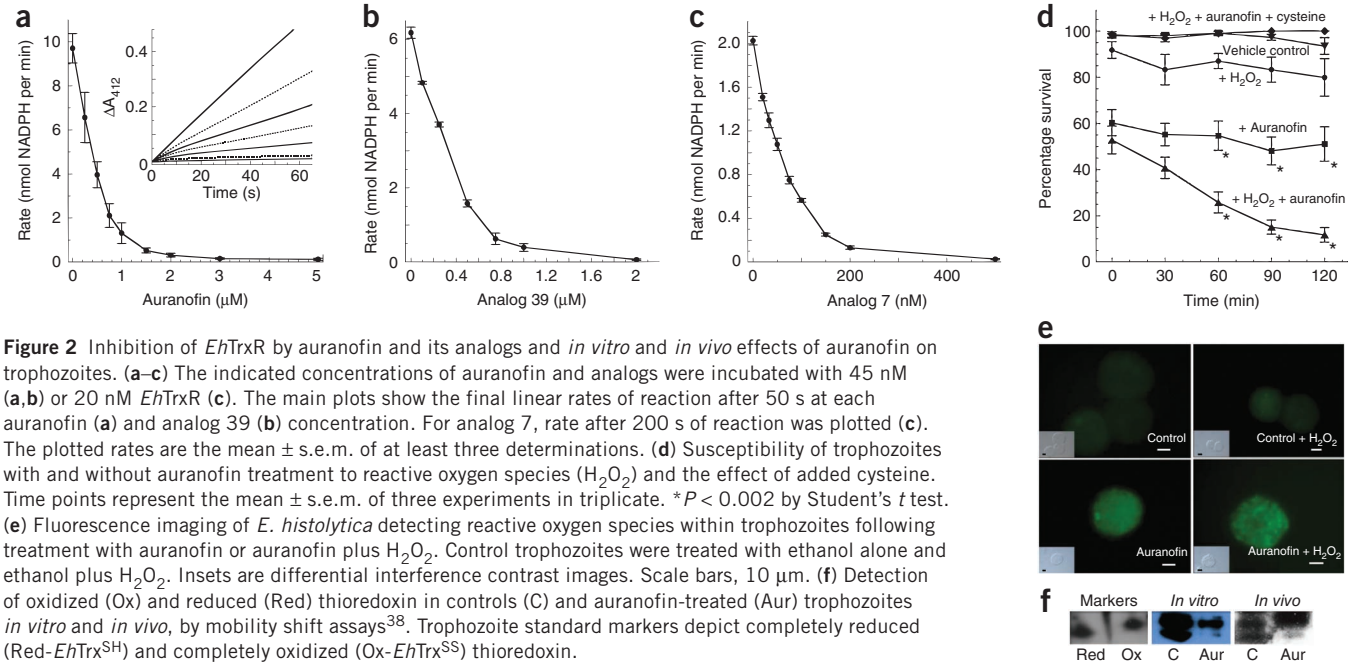

Figure 2 Inhibition of *Eh*TrxR by auranofin and its analogs and *in vitro* and *in vivo* effects of auranofin on trophozoites. (**a**–**c**) The indicated concentrations of auranofin and analogs were incubated with 45 nM (**a**,**b**) or 20 nM *Eh*TrxR (**c**). The main plots show the final linear rates of reaction after 50 s at each auranofin (**a**) and analog 39 (**b**) concentration. For analog 7, rate after 200 s of reaction was plotted (**c**). The plotted rates are the mean ± s.e.m. of at least three determinations. (**d**) Susceptibility of trophozoites with and without auranofin treatment to reactive oxygen species (H_2O_2) and the effect of added cysteine. Time points represent the mean ± s.e.m. of three experiments in triplicate. $^*P < 0.002$ by Student's *t* test. (**e**) Fluorescence imaging of *E. histolytica* detecting reactive oxygen species within trophozoites following treatment with auranofin or auranofin plus H_2O_2. Control trophozoites were treated with ethanol alone and ethanol plus H_2O_2. Insets are differential interference contrast images. Scale bars, 10 μm. (**f**) Detection of oxidized (Ox) and reduced (Red) thioredoxin in controls (C) and auranofin-treated (Aur) trophozoites *in vitro* and *in vivo*, by mobility shift assays[38]. Trophozoite standard markers depict completely reduced (Red-*Eh*Trx^{SH}) and completely oxidized (Ox-*Eh*Trx^{SS}) thioredoxin.

new gene in *E. histolytica* selectively inducible by auranofin exposure. It is noteworthy that both arsenite and auranofin are reported to be inhibitors of thioredoxin reductase (TrxR)[23,24] and metabolic inhibitors of selenium metabolism[25]. This led us to hypothesize that *E. histolytica* TrxR is the probable target of auranofin. Because *E. histolytica* resides in either aerobic (liver) or anaerobic (colon) environments in its mammalian hosts, the parasite must have a means to minimize damage caused by reactive oxygen species produced by the host immune assault. In most organisms, there are two largely independent systems to detoxify reactive oxygen species, one based on glutathione and the other based on thioredoxin. Each of these systems has a dedicated NADPH-dependent flavoenzyme, glutathione reductase and TrxR, to maintain the reduced state of glutathione and thioredoxin, respectively[26–28]. However, *E. histolytica* lacks both glutathione reductase activity and glutathione synthetic enzymes[29]; its TrxR is involved in prevention, intervention and repair of damage caused by oxidative stress[30].

There is a single TrxR-encoding gene in the *E. histolytica* genome (*EHI_155440*). *E. histolytica* TrxR (*Eh*TrxR) belongs to the low-molecular-weight TrxR family[31] and is similar to bacterial and yeast enzymes, including the TrxR from *Escherichia coli* (**Supplementary Fig. 2**). In contrast, most higher eukaryotes have a high-molecular-weight TrxR that is typically a selenocysteine protein; this enzyme in *S. mansoni*, known as TGR, has both selenium and an appended glutaredoxin domain[24] (**Supplementary Fig. 3**). We hypothesized that *Eh*TrxR would not contain selenium and that auranofin would bind the active-site cysteines. We were able to readily purify active, His-tagged *Eh*TrxR from solubilized *E. coli* by nickel-affinity chromatography[30] for use in inhibition studies.

We examined the activities of auranofin and its two most active analogs for inhibition of recombinant *Eh*TrxR. Low-micromolar concentrations of auranofin and analog 39 and nanomolar concentrations of analog 7 were inhibitory (**Fig. 2a–c**). The assays were nonlinear for the first 50 s (shown for auranofin in the inset of **Fig. 2a** at concentrations of 0, 0.25, 0.5, 0.75, 1, 2 and 5 μM, in order of decreasing slope), unlike control reactions without auranofin; inhibition increased with time until a linear, inhibited rate was established after 50 s of reaction (**Fig. 2a**). Examination of the rates after 50 s indicated that 0.4 μM auranofin caused 50% inhibition. The EC_{50} values for analog 39 and analog 7 were 0.33 and 0.055 μM, respectively. Preincubation of the inhibitor with reduced *Eh*TrxR did not remove the lag phase in inhibition, as seen by the nonlinearity of the data acquired up to 50 s (data not shown).

Because TrxR is crucial for protecting amebic trophozoites from oxidant attack, we compared the susceptibility of trophozoites with and without auranofin treatment to reactive oxygen species (H_2O_2). After incubation of trophozoites with 2 μM auranofin for 18 h, the remaining viable trophozoites (~50%) were significantly more sensitive to killing by 300 μM H_2O_2 than control trophozoites in medium alone ($P < 0.002$) (**Fig. 2d**). Killing by auranofin (2 μM) and H_2O_2 was reversed by the presence of 2 mg ml^{-1} of cysteine (**Fig. 2d**). Cysteine is the major reductant in *E. histolytica*[32], and its apparent protective effect may be through direct reduction of thioredoxin or inhibition of auranofin binding to cysteine residues in TrxR. We detected the presence of reactive oxygen species after 2 μM auranofin treatment with fluorescence generated by the oxidation of dichlorodihydrofluorescein added to the medium[33] (**Fig. 2e**). However, the same concentration of metronidazole, although producing stress, did not increase intracellular reactive oxygen species (**Supplementary Fig. 4**). Moreover, we observed increased amounts of oxidized thioredoxin in auranofin-treated trophozoites, both *in vitro* and *in vivo*, indicating that TrxR may be a target for auranofin (**Fig. 2f**).

Recently, the crystal structure of *S. mansoni* TGR that had been incubated with auranofin before crystallization was solved[24]. The structure revealed gold (Au(I)) rather than auranofin as an adduct between pairs of cysteines (Cys-Au-Cys) in two different sites and also bound to the proposed NADPH binding site of the reductase in a third location. The C terminus of TGR containing a selenocysteine residue was not observed in the structure and may have bound a fourth gold atom. The authors of that study proposed that the selenocysteine at the penultimate position of TGR accelerated the release of gold from auranofin to form the inactivated enzymes; benzeneselenol added to a

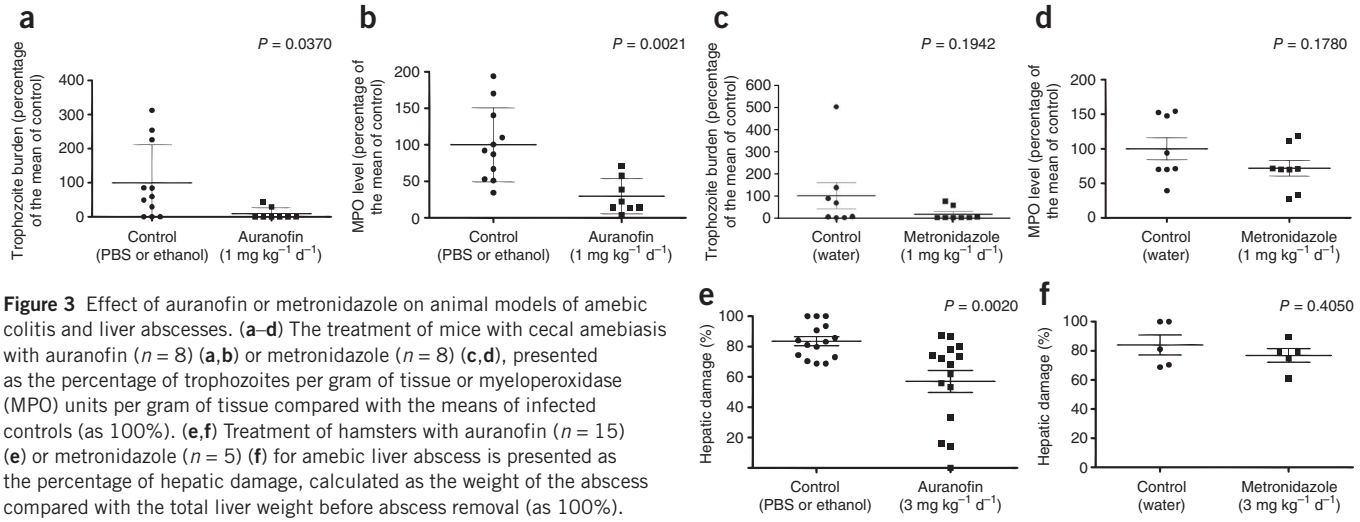

Figure 3 Effect of auranofin or metronidazole on animal models of amebic colitis and liver abscesses. (**a**–**d**) The treatment of mice with cecal amebiasis with auranofin ($n = 8$) (**a**,**b**) or metronidazole ($n = 8$) (**c**,**d**), presented as the percentage of trophozoites per gram of tissue or myeloperoxidase (MPO) units per gram of tissue compared with the means of infected controls (as 100%). (**e**,**f**) Treatment of hamsters with auranofin ($n = 15$) (**e**) or metronidazole ($n = 5$) (**f**) for amebic liver abscess is presented as the percentage of hepatic damage, calculated as the weight of the abscess compared with the total liver weight before abscess removal (as 100%).

C-terminally truncated TGR or to glutathione reductase increased the rate of inactivation by auranofin[24]. The crystal structure of reduced *L. infantum* trypanothione reductase complexed with NADPH and auranofin also demonstrated that gold binds two active cysteine residues of trypanothione reductase[16].

*Eh*TrxR is of very similar size and domain topology as *E. coli* TrxR, a well-studied enzyme[34]. Both proteins have an active site dithiol/disulfide center (Cys-Ala-Thr-Cys for *Ec*TrxR, Cys-Ala-Ile-Cys for *Eh*TrxR) plus either two or four additional cysteine residues, respectively (**Supplementary Fig. 2**). By analogy with the *S. mansoni* TGR, addition of auranofin could cause gold atoms to bind the NADPH-binding site of *Eh*TrxR, the active-site thiols, the four cysteine residues near the C terminus of the enzyme or some combination of these sites.

Because of auranofin's *in vitro* activity against *E. histolytica* trophozoites and oral availability, we tested its efficacy in two animal models of amebiasis. We adapted a mouse amebic colitis model in which trophozoites invade and colonize mouse cecal tissue after surgical inoculation[35,36]. We co-cultured amebic trophozoites with cecal bacteria and surgically inoculated them into the cecum of C3H/HeJ mice. We delivered auranofin or metronidazole by gavage 24 h after infection at a concentration of 1 mg per kg body weight per day for 7 d (ref. 37). Both the parasite burden and the inflammatory response as measured by activity of myeloperoxidase in cecal tissue were significantly decreased by auranofin ($P = 0.037$ and $P = 0.0021$, respectively) (**Fig. 3a**,**b**) but not by metronidazole (**Fig. 3c**,**d**). Auranofin (**Fig. 3e**) was more effective than an equivalent dose of metronidazole (**Fig. 3f**) in a hamster model of amebic liver abscess where treatment started 4 d after infection. A single oral dose of 3 mg per kg body weight per day of auranofin for 7 d significantly decreased hepatic damage in hamsters ($P = 0.002$) (**Fig. 3e**). These findings suggest that auranofin may be an entirely new class of drug to treat amebiasis and potentially other parasitic infections. On the basis of these results, the FDA has approved an orphan-drug designation of auranofin for treatment of amebiasis.

In summary, we have shown that it is feasible to screen large numbers of compounds in an HTS format for effectiveness against *E. histolytica*, and robust and reproducible results can be generated from this HTS. The discovery of the amebicidal activity of the FDA-approved drug auranofin offers a promising drug-repositioning opportunity for the treatment of amebiasis.

METHODS

Methods and any associated references are available in the online version of the paper.

Accession codes. Microarray data are deposited in ArrayExpress with accession code E-MEXP-3494.

Note: Supplementary information is available in the online version of the paper.

ACKNOWLEDGMENTS

This work was supported by the Sandler Foundation and US National Institute of Allergy and Infectious Diseases grant 5U01AI077822; we also acknowledge support from R01 GM050389. *E. histolytica* microarray slides were kindly provided by S.L. Stanley Jr. (Stony Brook University, New York), and the *E. histolytica* thioredoxin–specific antibody was a kind gift from S. Adrian-Guerrero (Universidad Nacional del Litoral). We thank G. Hwang and C. Le for their help with the mouse surgery and K. Ang and J. Gut for sharing their expertise.

AUTHOR CONTRIBUTIONS

A.D. and J.H.M. designed the HTS screening studies and arrays. A.D. performed HTS and array experiments. D.P. and L.B.P. performed the enzymatic assays. R.M.A. performed the oxidant studies. C.H., E.R.C., K.H., G.G.-R., E.O. and M.B.M. did the *in vivo* studies. K.H. purified recombinant *Eh*TrxR. S.C. and M.R.A. provided compound libraries and edited the manuscript. S.S.G. and A.M.B. synthesized auranofin analogs. S.L.R. designed the *Eh*TrxR and oxidant studies. A.D., L.B.P., J.H.M. and S.L.R. wrote the manuscript.

COMPETING FINANCIAL INTERESTS

The authors declare no competing financial interests.

Published online at http://www.nature.com/doifinder/10.1038/nm.2758.
Reprints and permissions information is available online at http://www.nature.com/reprints/index.html.

1. World Health Organization. The World Health Report 1998: life in the 21st century: a vision for all. <http://www.who.int/whr/1998/en/whr98_en.pdf> (1998).
2. Freeman, C.D., Klutman, N.E. & Lamp, K.C. Metronidazole. A therapeutic review and update. *Drugs* **54**, 679–708 (1997).
3. Krogstad, D.J. & Cedeno, J.R. Problems with current therapeutic regimens. in *Amebiasis: Human Infection by Entamoeba Histolytica* (ed. Ravdin, J.I.) 741–748 (John Wiley & Sons, New York, 1988).
4. Samarawickrema, N.A., Brown, D.M., Upcroft, J.A., Thammapalerd, N. & Upcroft, P. Involvement of superoxide dismutase and pyruvate:ferredoxin oxidoreductase in mechanisms of metronidazole resistance in *Entamoeba histolytica*. *J. Antimicrob. Chemother.* **40**, 833–840 (1997).
5. Wassmann, C., Hellberg, A., Tannich, E. & Bruchhaus, I. Metronidazole resistance in the protozoan parasite *Entamoeba histolytica* is associated with increased expression of iron-containing superoxide dismutase and peroxiredoxin and decreased expression of ferredoxin 1 and flavin reductase. *J. Biol. Chem.* **274**, 26051–26056 (1999).

6. Seifert, K. *et al.* Effects of miltefosine and other alkylphosphocholines on human intestinal parasite *Entamoeba histolytica*. *Antimicrob. Agents Chemother.* **45**, 1505–1510 (2001).
7. Ghosh, S. *et al.* Effects of bisphosphonates on the growth of *Entamoeba histolytica* and *Plasmodium* species *in vitro* and *in vivo*. *J. Med. Chem.* **47**, 175–187 (2004).
8. Singh, S., Athar, F. & Azam, A. Synthesis, spectral studies and in vitro assessment for antiamoebic activity of new cyclooctadiene ruthenium(II) complexes with 5-nitrothiophene-2-carboxaldehyde thiosemicarbazones. *Bioorg. Med. Chem. Lett.* **15**, 5424–5428 (2005).
9. Ashburn, T.T. & Thor, K.B. Drug repositioning: identifying and developing new uses for existing drugs. *Nat. Rev. Drug Discov.* **3**, 673–683 (2004).
10. Makioka, A., Kumagai, M., Ohtomo, H., Kobayashi, S. & Takeuchi, T. Effect of calcium antagonists, calcium channel blockers and calmodulin inhibitors on the growth and encystation of *Entamoeba histolytica* and *E. invadens*. *Parasitol. Res.* **87**, 833–837 (2001).
11. Gottlieb, N.L. Pharmacology of auranofin: overview and update. *Scand. J. Rheumatol. Suppl.* **63**, 19–28 (1986).
12. Kuntz, A.N. *et al.* Thioredoxin glutathione reductase from *Schistosoma mansoni:* an essential parasite enzyme and a key drug target. *PLoS Med.* **4**, e206 (2007).
13. Lobanov, A.V., Gromer, S., Salinas, G. & Gladyshev, V.N. Selenium metabolism in *Trypanosoma*: characterization of selenoproteomes and identification of a kinetoplastida-specific selenoprotein. *Nucleic Acids Res.* **34**, 4012–4024 (2006).
14. Bonilla, M. *et al.* Platyhelminth mitochondrial and cytosolic redox homeostasis is controlled by a single thioredoxin glutathione reductase and dependent on selenium and glutathione. *J. Biol. Chem.* **283**, 17898–17907 (2008).
15. Sannella, A.R. *et al.* New uses for old drugs. Auranofin, a clinically established antiarthritic metallodrug, exhibits potent antimalarial effects *in vitro*: Mechanistic and pharmacological implications. *FEBS Lett.* **582**, 844–847 (2008).
16. Ilari, A. *et al.* A gold-containing drug against parasitic polyamine metabolism: the X-ray structure of trypanothione reductase from *Leishmania infantum* in complex with auranofin reveals a dual mechanism of enzyme inhibition. *Amino Acids* **42**, 803–811 (2012).
17. Davis, P.H., Schulze, J. & Stanley, S.L. Jr. Transcriptomic comparison of two *Entamoeba histolytica* strains with defined virulence phenotypes identifies new virulence factor candidates and key differences in the expression patterns of cysteine proteases, lectin light chains and calmodulin. *Mol. Biochem. Parasitol.* **151**, 118–128 (2007).
18. Blower, M.D., Nachury, M., Heald, R. & Weis, K.A. Rae1-containing ribonucleoprotein complex is required for mitotic spindle assembly. *Cell* **121**, 223–234 (2005).
19. Parks, R.E. Jr. *et al.* Purine metabolism in primitive erythrocytes. *Comp. Biochem. Physiol. B* **45**, 355–364 (1973).
20. Créchet, J.B., Cool, R.H., Jacquet, E. & Lallemand, J.Y. Characterization of *Saccharomyces cerevisiae* Ras1p and chimaeric constructs of Ras proteins reveals the hypervariable region and farnesylation as critical elements in the adenylyl cyclase signaling pathway. *Biochemistry* **42**, 14903–14912 (2003).
21. Arnaud-Dabernat, S. *et al.* Nm23-M2/NDP kinase B induces endogenous c-myc and nm23-M1/NDP kinase A overexpression in BAF3 cells. Both NDP kinases protect the cells from oxidative stress-induced death. *Exp. Cell Res.* **301**, 293–304 (2004).
22. Sok, J. *et al.* Arsenite-inducible RNA-associated protein (AIRAP) protects cells from arsenite toxicity. *Cell Stress Chaperones* **6**, 6–15 (2001).
23. Lu, J., Chew, E.H. & Holmgren, A. Targeting thioredoxin reductase is a basis for cancer therapy by arsenic trioxide. *Proc. Natl. Acad. Sci. USA* **104**, 12288–12293 (2007).
24. Angelucci, F. *et al.* Inhibition of *Schistosoma mansoni* thioredoxin-glutathione reductase by auranofin: structural and kinetic aspects. *J. Biol. Chem.* **284**, 28977–28985 (2009).
25. Talbot, S., Nelson, R. & Self, W.T. Arsenic trioxide and auranofin inhibit selenoprotein synthesis: implications for chemotherapy for acute promyelocytic leukaemia. *Br. J. Pharmacol.* **154**, 940–948 (2008).
26. Townsend, D.M., Tew, K.D. & Tapiero, H. The importance of glutathione in human disease. *Biomed. Pharmacother.* **57**, 145–155 (2003).
27. Lillig, C.H. & Holmgren, A. Thioredoxin and related molecules—from biology to health and disease. *Antioxid. Redox Signal.* **9**, 25–47 (2007).
28. Sayed, A.A. *et al.* Identification of oxadiazoles as new drug leads for the control of schistosomiasis. *Nat. Med.* **14**, 407–412 (2008).
29. Fahey, R.C., Newton, G.L., Arrick, B., Overdank-Bogart, T. & Aley, S.B. *Entamoeba histolytica:* a eukaryote without glutathione metabolism. *Science* **224**, 70–72 (1984).
30. Arias, D.G., Gutierrez, C.E., Iglesias, A.A. & Guerrero, S.A. Thioredoxin-linked metabolism in *Entamoeba histolytica*. *Free Radic. Biol. Med.* **42**, 1496–1505 (2007).
31. Hirt, R.P., Muller, S., Embley, T.M. & Coombs, G.H. The diversity and evolution of thioredoxin reductase: new perspectives. *Trends Parasitol.* **18**, 302–308 (2002).
32. Jeelani, G. *et al.* Two atypical L-cysteine-regulated NADPH-dependent oxidoreductases involved in redox maintenance, L-cystine and iron reduction and metronidazole activation in the enteric protozoan *Entamoeba histolytica*. *J. Biol. Chem.* **285**, 26889–26899 (2010).
33. Sen, A., Chatterjee, N.S., Akbar, M.A., Nandi, N. & Das, P. The 29-kilodalton thiol-dependent peroxidase of *Entamoeba histolytica* is a factor involved in pathogenesis and survival of the parasite during oxidative stress. *Eukaryot. Cell* **6**, 664–673 (2007).
34. Williams, C.H. *et al.* Thioredoxin reductase: two modes of catalysis have evolved. *Eur. J. Biochem.* **267**, 6110–6117 (2000).
35. Houpt, E.R. *et al.* The mouse model of amebic colitis reveals mouse strain susceptibility to infection and exacerbation of disease by $CD4^+$ T cells. *J. Immunol.* **169**, 4496–4503 (2002).
36. He, C. *et al.* A novel *Entamoeba histolytica* cysteine proteinase, EhCP4, is key for invasive amebiasis and a therapeutic target. *J. Biol. Chem.* **285**, 18516–18527 (2010).
37. Markiewicz, V.R., Saunders, L.A., Geus, R.J., Payne, B.J. & Hook, J.B. Carcinogenicity study of auranofin, an orally administered gold compound in mice. *Fundam. Appl. Toxicol.* **11**, 277–284 (1988).
38. Bersani, N.A., Merwin, J.R., Lopez, M.I., Pearson, G.D. & Merrill, G.F. Protein electrophoretic mobility shift assay to monitor redox state of thioredoxin in cells. *Methods Enzymol.* **347**, 317–326 (2002).

ONLINE METHODS

***E. histolytica* cultures.** Axenic *E. histolytica* (HM1:IMSS) trophozoites were maintained in TYI-S-33 medium[39] and counted using a particle counter (Beckman Coulter).

Compound libraries. A library of 910 bioactive compounds was donated by Iconix Biosciences.

HTS cell viability assay. Compounds were diluted using a Biomek FX^P Laboratory Automation Workstation (Beckman Coulter) and the Matrix WellMate bulk dispenser (Thermo Fisher Scientific) to yield 125 µM compound in 12.5% DMSO. Finally, FX^P transferred 4 µL of diluted compound to the 96-well screen plates, followed by addition of 96 µL (5,000 parasites) of *E. histolytica* trophozoites in TYI-S-33 complete medium to the 96-well plates by the WellMate. Final concentrations of test compound and DMSO per well were 5 µM and 0.5%, respectively.

Negative controls in the screen plates contained 0.5% DMSO, and positive controls contained 30 µM metronidazole (Sigma). Assay plates were incubated for 48 h at 37 °C in the GasPak (VWR) to maintain an anaerobic condition throughout the incubation period. At the end of incubation, the assay plates were equilibrated to room temperature for 30 min, and 50 µL of CellTiter-Glo (Promega) was added in each well of the 96-well plates using the WellMate. The plates were then placed on an orbital shaker at room temperature for 10 min to induce cell lysis. After lysis, the plates were again equilibrated at room temperature for 10 min to stabilize the luminescent signal. The resulting ATP bioluminescence of the trophozoites was measured at room temperature using an Analyst HT plate reader (Molecular Devices).

Secondary screen for potency determination. For confirmatory screens of trophozoites, hits from the primary screen were picked from 5-mM stocks in 100% DMSO using the Biomek FX^P. For eight-point EC_{50} determination experiments, we diluted 2.5 µL of stock compounds with 17.5 µL sterile water to yield 625 µM working concentration of library compounds. A threefold serial dilution was then performed yielding a concentration range of 0.25–625 µM. From this dilution plate, 4 µL were transferred into the 96-well screen plates followed by addition of 96 µL of trophozoites (5,000 parasites) to yield a final eight-point concentration range spanning 0.01–25 µM in final 0.5% DMSO. The assays were performed in triplicate using CellTiter-Glo. Visualization and statistical analysis of secondary screening were performed using GraphPad Prism software 4.0.

HTS data analysis and statistics. The raw data file from the Analyst HT plate reader was uploaded using Pipeline Pilot 4.5.2 into Small Molecule Discovery Center's database. The results of the data analysis are provided in **Supplementary Data 1** and **2**. Percentage inhibition relative to maximum and minimum reference signal controls was calculated using the formula: percentage inhibition = ((mean of maximum signal reference control – experimental value)/(mean of maximum signal reference control – mean of minimum signal reference control)) × 100.

The cutoff was selected to determine actives from the primary screen, which was at least 50% inhibition and 3 s.d. above the mean of the population of compounds tested.

***E. histolytica* microarray analysis.** We used *E. histolytica* oligonucleotide arrays for characterizing transcriptional effects of auranofin. These microarrays were composed of 6,209 70-mer oligonucleotides and encompassed approximately 90% of the unique genes found in the *E. histolytica* genome data set as of February 2004. Oligonucleotides were printed in triplicate on slides by the Washington University School of Medicine Microarray Core Facility[17]. We used Trizol (Invitrogen) to isolate total RNA from 2×10^6 *E. histolytica* HM1:IMSS treated for 3 h with 0.5% DMSO and 2×10^6 *E. histolytica* HM1:IMSS treated for 3 h with 1 µM auranofin. Total RNA was amplified with the Amino Allyl MessageAmp II aRNA Amplification Kit (Ambion) following the manufacturer's protocol. The monofunctional NHS-ester Cy3 and Cy5 dyes (GE Healthcare Life Sciences) were coupled with 10 µg amplified RNA. The two amplified RNA pools to be compared were mixed and applied to *E. histolytica* microarray. Four samples (two from DMSO-treated and two from auranofin-treated *E. histolytica*) were competitively hybridized on two individual chips. The hybridization was performed at 63 °C for 16 h in a humidified slide chamber containing the labeled probe, 3× saline sodium citrate (SSC) and 0.2% SDS. After hybridization, the hybridization chamber was removed from the 63 °C water bath, washed with 0.6× SSC, 0.03% SDS and then 0.06× SSC. Microarrays were scanned using a GenePix Pro Axon 4000B scanner, and then data were analyzed (Acuity software, Molecular Devices) and deposited in the public database ArrayExpress.

Quantitative real-time PCR. We isolated total RNA from control and auranofin-treated trophozoites as described under *E. histolytica* microarray analysis (above). After reverse transcription, we performed qRT-PCR using SYBR Green I Master (Roche Applied Science), and the PCR product was monitored (Mx3005P QPCR System with MxPro QPCR software, Stratagene). Primer sequences are in **Supplementary Table 3**.

Purification of recombinant *E. histolytica* TrxR. The *Eh*TrxR coding sequence was amplified[30] from genomic DNA[36], cloned into pET22b (Novagen) and transformed into BL21 Codon Plus cells (Stratagene). Protein expression was induced (1 mM IPTG, 2 h, 37 °C), the pellet was lysed in Bacterial Protein Extraction Reagents (B-PER) (Thermo Scientific) and soluble *Eh*TrxR (1% Triton X-100, 10 mM imidazole) was purified by NiNTA affinity chromatography (Qiagen).

***E. histolytica* TrxR assay.** The thionitrobenzoate-coupled assay for TrxR activity was modified from Mulrooney[40]. Briefly, 600 µL total of 50 mM potassium phosphate, pH 7.0, 1 mM EDTA contained 20 µM *E. coli* Trx1, 200 µM 5,5′-dithiobis(2-nitrobenzoic acid) (DTNB) and 20 or 45 nM *Eh*TrxR at 25 °C. The reaction was started by addition of 100 µM NADPH and monitored by absorbance at 412 nm, which increases with the reaction due to DTNB reduction. With these concentrations of DTNB and *Eh*TrxR, in the absence of *Ec*TrxA there was a negligible increase in absorbance at 412 nm. When present, different concentrations of auranofin (predissolved in ethanol) were added 3 min before the NADPH (to a maximum added volume, at 3.6 µL, of 0.6% of the total). The initial rate and the rate after 50 s were calculated from the increase in absorbance at 412 nm, using an extinction coefficient for nitrothiobenzoate anion of 13,600 M^{-1} cm^{-1} (with two molecules of nitrothiobenzoate generated per NADPH oxidized) to convert the absorbance change to rates in nmol NADPH per min.

Auranofin effect on trophozoites. To determine the effect of auranofin on oxidant stress, we preincubated trophozoites (5×10^5 in TYI-S-33) at 37 °C with auranofin (2 µM, 18 h), ethanol or TYI-S-33 containing 2 mg mL^{-1} of cysteine (Sigma). Trophozoites were then counted, resuspended in TYI-S-33 with 300 µM H_2O_2 and their viability was assessed by Trypan blue exclusion. Aliquots were removed in triplicate every 30 min for 2 h and percentage survival determined with the CellTiter-Glo, with statistical analysis by Student's *t* test.

We determined intracellular oxidant levels by incubating control trophozoites (treated with ethanol), trophozoites treated with ethanol plus H_2O_2, trophozoites treated with auranofin and trophozoites treated with auranofin plus H_2O_2 with 0.2 mM 2′,7′-dichlorodihydro-fluorescein diacetate (Sigma) for 45 min (ref. 33), washing, fixing with 4% paraformaldehyde, resuspending in ProLong Gold mounting medium with nuclear stain (DAPI) and examining by a Nikon E800 fluorescence microscope.

The redox state of thioredoxin in amebic trophozoites was determined by protein electrophoretic mobility shift assay[38]. HM1:IMSS trophozoites were incubated 18 h with auranofin (2 µM) or medium alone. *In vivo* trophozoites were obtained by flushing infected mouse cecum after treatment for 48 h with auranofin at 1 mg per kg body weight or the ethanol vehicle alone. Trophozoites were washed in PBS, pH 7.4, lysed in 100 mM Tris, 8 M urea, 1 mM EDTA and 30 mM iodoacetic acid, pH 7.2, for 37 °C for 15 min; excess iodoacetic acid was removed by precipitation in cold acetone with 1 N HCl (98:2, v/v) and washed in acetone with 1 N HCl and water (98:2:10). The disulfides were subsequently reduced in the urea buffer containing 3.5 mM DTT for 30 min at 37 °C, and the new thiols amidomethylated with 10 mM iodoacetamide. Markers were prepared

doi:10.1038/nm.2758

by incubating cultured trophozoites in urea buffer with 3.5 mM DTT for 30 min at 37 °C, then equal aliquots alkylated with 30 mM iodoacetic acid (reduced marker) or 10 mM iodoacetamide (oxidized) marker for 30 min at 37 °C (ref. 38). Samples were electrophoresed by native urea-PAGE on 9% gels and transferred to nitrocellulose; the bands were detected with rabbit *Eh*Trx-specific antibody[30] (1:200, a gift from S. Adrian-Guerrero) and goat antibody to rabbit IgG conjugated to horseradish peroxidase (Invitrogen, 1:10,000, catalog no. 65-6120) by enhanced chemiluminescence (SuperSignal, West Pico, Fisher Scientific).

***In vivo* efficacy of auranofin.** We injected cecal-passed trophozoites into the externalized cecum of 6-week-old C3H/HeJ male mice[35] (Jackson Laboratory) and treated them orally 24 h after infection with 1 mg per kg body weight per day auranofin (Enzo Life Sciences) or metronidazole for 7 d. The mice were then killed, and the cecum was removed for histopathology. Trophozoites were quantified by real-time PCR, and myeloperoxidase activity was assayed[41]. Mouse studies were approved by the University of California–San Diego Institutional Animal Care Committee.

We injected trophozoites (250,000 in 0.2 mL TYI-S-33) intraportally in hamsters to induce liver abscesses. The hamsters were treated 4 d after infection orally with 3 mg per kg body weight of auranofin, metronidazole or PBS daily for 7 d. The hamsters were killed, and the livers and abscesses were dissected and weighed. Hamster studies were approved by the Centro de Investigación y de Estudios Avanzados del Instituto Politécnico Nacional Internal Committee for the Care and Use of the Laboratory Animals.

39. Diamond, L.S., Harlow, D.R. & Cunnick, C.C. A new medium for the axenic cultivation of *Entamoeba histolytica* and other *Entamoeba*. *Trans. R. Soc. Trop. Med. Hyg.* **72**, 431–432 (1978).
40. Mulrooney, S.B. Application of a single-plasmid vector for mutagenesis and high-level expression of thioredoxin reductase and its use to examine flavin cofactor incorporation. *Protein Expr. Purif.* **9**, 372–378 (1997).
41. Meléndez-López, S.G. *et al.* Use of recombinant *Entamoeba histolytica* cysteine proteinase 1 to identify a potent inhibitor of amebic invasion in a human colonic model. *Eukaryot. Cell* **6**, 1130–1136 (2007).